Holographic Storage of Biphoton Entanglement

Han-Ning Dai,[1] Han Zhang,[1] Sheng-Jun Yang,[1] Tian-Ming Zhao,[1] Jun Rui,[1] You-Jin Deng,[1] Li Li,[1,*] Nai-Le Liu,[1] Shuai Chen,[1] Xiao-Hui Bao,[2,1] Xian-Min Jin,[1] Bo Zhao,[1,3,†] and Jian-Wei Pan[1]

[1]*Hefei National Laboratory for Physical Sciences at Microscale and Department of Modern Physics, University of Science and Technology of China, Hefei, Anhui 230026, China*

[2]*Physikalisches Institut, Reprecht-Karls-Universitat Heidelberg, Philosophenweg 12, 69120 Heidelberg, Germany*

[3]*Institute for Theoretical Physics, University of Innsbruck, A-6020 Innsbruck, Austria*

(Received 16 February 2012; revised manuscript received 20 March 2012; published 21 May 2012)

Coherent and reversible storage of multiphoton entanglement with a multimode quantum memory is essential for scalable all-optical quantum information processing. Although a single photon has been successfully stored in different quantum systems, storage of multiphoton entanglement remains challenging because of the critical requirement for coherent control of the photonic entanglement source, multimode quantum memory, and quantum interface between them. Here we demonstrate a coherent and reversible storage of biphoton Bell-type entanglement with a holographic multimode atomic-ensemble-based quantum memory. The retrieved biphoton entanglement violates the Bell inequality for 1 μs storage time and a memory-process fidelity of 98% is demonstrated by quantum state tomography.

DOI: 10.1103/PhysRevLett.108.210501 PACS numbers: 03.67.Bg, 37.10.Gh, 42.50.Ex, 42.65.Lm

Faithfully mapping multiphoton entanglement into and out of quantum memory is of crucial importance for scalable linear-optical quantum computation [1] and long-distance quantum communication [2]. Recently, storage of nonclassical light [3,4] and single photons [5–12] has been demonstrated in various quantum systems, such as an atomic ensemble, solid system, and single atom. Among these, the atomic-ensemble-based quantum memory holds the promise to implement multimode quantum memory for multiphoton entanglement. A natural method for this purpose is to select spatially separated subensembles of a large atomic ensemble as different quantum registers [8,13], for which the number of stored modes is limited by the spatial dimension of the atomic ensemble. More powerful methods, such as exploring the large optical depth of an atomic ensemble [14,15], or utilizing photon echoes [16] or atomic frequency combs techniques [17], have been employed to demonstrate atomic-ensemble-based multimode memories.

An alternative and elegant method is to implement the atomic ensemble as a holographic multimode quantum memory [18–20], using spatially overlapped but orthogonal spin waves as different quantum registers. For clarity, we illustrate this in the example of storing a single-photon state in an atomic ensemble of N atoms that have two long-lived ground states $|g\rangle$ and $|s\rangle$ [21–24]. Initially, a ''vacuum'' state $|\mathrm{vac}\rangle = |g_1 \ldots g_N\rangle$ is prepared such that all the atoms are at the $|g\rangle$ state. The single-photon state is then mapped into the ensemble as a collective state $|1, \mathbf{q}\rangle = S_{\mathbf{q}}^{\dagger}|\mathrm{vac}\rangle = (1/\sqrt{N})\sum_j e^{i\mathbf{q}\cdot\mathbf{x}_j}|g_1 \cdots s_j \cdots g_N\rangle$, where $\mathbf{x}_j$ is the position of the jth atom, $S_{\mathbf{q}}^{\dagger} = (1/\sqrt{N})\sum_j e^{i\mathbf{q}\cdot\mathbf{x}_j}|s\rangle_j\langle g|$ is the collective creation operator of a spin wave with wave vector $\mathbf{q}$. For $N \gg 1$, one has $[S_{\mathbf{q}_1}, S_{\mathbf{q}_2}^{\dagger}] \approx \delta_{\mathbf{q}_1\mathbf{q}_2}$, namely, the collective states satisfy the orthogonality relation $\langle 1, \mathbf{q}_1|1, \mathbf{q}_2\rangle \approx \delta_{\mathbf{q}_1\mathbf{q}_2}$. Therefore, one can encode different qubits by different phase patterns and employ a single atomic ensemble as a holographic multimode quantum memory. Since the information is stored globally throughout the medium, one can achieve high-capacity data storage. Recently, holographic storage of classical light and microwave pulses has been demonstrated [25–27].

Here we report an experimental demonstration of holographic storage of biphoton Bell-type entanglement with a single atomic ensemble, in which four orthogonal spin waves with different wave vectors are used as a quad-mode quantum memory. The posterior biphoton entanglement is mapped into and out of the quad-register holographic quantum memory, via a technique based on electromagnetically induced transparency (EIT). Violation of the Bell inequality is observed for storage time up to 1 μs and a memory-process fidelity of 98%, calculated by quantum state tomography, is achieved.

The experimental scheme and setup are shown in Figs. 1 and 2, respectively. In the memory lab, we prepare, within 14 ms, a cold ^{87}Rb atomic ensemble consisting of about 10^8 atoms in a dark magnetic optical trap (MOT). The temperature of the atomic cloud is about 140 μK, and the optical depth is about 10. The typical Λ-type energy-level configuration is shown in Fig. 1(b), where $|g\rangle$, $|e\rangle$, and $|s\rangle$ correspond to the ^{87}Rb hyperfine states $|5S_{1/2}, F = 1\rangle$, $|5P_{1/2}, F = 2\rangle$, and $|5S_{1/2}, F = 2\rangle$, respectively. All the atoms are initially prepared at $|g\rangle$.

A strong classical control field couples $|e\rangle$-$|s\rangle$ transition with wave vector $\mathbf{k}_c$ and beam waist diameter $w_c \approx 850$ μm, while the to-be-stored quantum field, which has four components (see below), couples the $|g\rangle$-$|e\rangle$ transition with beam waist diameter $w_s \approx 450$ μm. The control field is focused at the ensemble center, and the four components

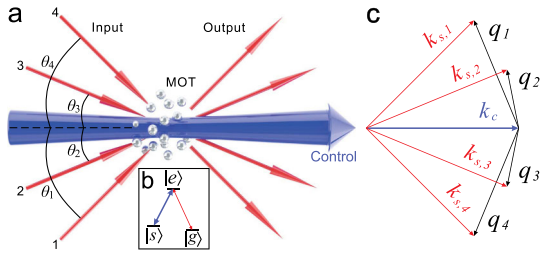

FIG. 1 (color online). (a) Schematic view of the quad-mode holographic quantum memory. The control field is shined into the atomic cloud horizontally, and the signal modes are incident from different directions in the same plane, with angles $(\theta_1, \theta_2, \theta_3, \theta_4) = (-1°, -0.6°, 0.6°, 1°)$ relative to the control field. (b) Typical Λ-type energy levels, with two ground states $|g\rangle$ and $|s\rangle$ and an excited state $|e\rangle$. The $|e\rangle$-$|g\rangle$ and the $|e\rangle$-$|s\rangle$ transition are coupled to the signal and control fields, respectively. (c) Illustration of the wave vectors of the spin waves. The input signal field with a wave vector of $\mathbf{k}_{s,i}$ $(i = 1, 2, 3, 4)$ is mapped to a spin wave with the wave vector $\mathbf{q}_i = \mathbf{k}_{s,i} - \mathbf{k}_c$, with $\mathbf{k}_c$ the wave vector of the control field.

of the signal field are guided through the atomic cloud along four different directions, which are in the same plane but with different angles $\theta_i (i = 1 - 4)$ relative to the control-light direction [28]. We set $(\theta_1, \theta_2, \theta_3, \theta_4) = (-1°, -0.6°, 0.6°, 1°)$, as illustrated in Fig. 1(a). By carefully adjusting the directions of the control and signal beams, we make all the light modes overlap in the center of the atomic ensemble. The atomic ensemble has a length $L \approx 2$ mm, and the signal fields propagate within the control field during storage.

Each component i of the signal field is associated with a wave vector $\mathbf{k}_{s,i}$, and is to be stored in a spin wave with $\mathbf{q}_i = \mathbf{k}_{s,i} - \mathbf{k}_c$. By careful alignment, a holographic quad-mode quantum memory, with approximately equivalent optical depth and similar performance, is established. We measure the EIT transmission spectrum and perform a slow-light experiment. For a control light with a Rabi frequency of about 7 MHz, we observe an EIT window of 2.2 MHz and a delay time of about 160 ns for all the four modes. Note that such a holographic quantum memory is different from the scheme in Refs. [8,13], where each signal mode requests a spatially separated atomic subensemble.

The biphoton entanglement comes from a narrowband cavity-enhanced spontaneous parametric down-conversion (SPDC) entanglement source as in previous work [9,29]. The source cavity contains three main parts, i.e., a nonlinear crystal, a tuning crystal, and an output coupler. The nonlinear crystal is a 25 mm type-II periodically poled $KTiOPO_4$ (PPKTP) crystal, whose operational wavelength $\lambda \approx 795$ nm is designed to match the $D1$ transition line of ^{87}Rb. The cavity is locked intermittently to a Ti:sapphire laser using the Pound-Drever-Hall method. The linewidth and finesse of the cavity are measured to be 5 MHz and 170, respectively.

Polarization-perpendicular photon pairs are created by applying a ultraviolet (UV) pumping light, which is up converted from the Ti:sapphire laser. Single-mode output is achieved by using a filter cavity (made of a single piece of fused silica of about 6.35 mm) with a finesse of 30, which removes the background modes. Polarization-entangled photon pairs are postselected by interfering the twin photons at the polarization beam splitters (PBSs). The ideal outcome state corresponds to a Bell state

$$|\phi^+\rangle_p = (|H\rangle_1|H\rangle_2 + |V\rangle_1|V\rangle_2)/\sqrt{2}$$

where $H(V)$ represents the horizontal (vertical) polarization of the photons. Under a continuous wave (cw) pump with a pump power of 4 mW, the spectrum brightness of the polarization-entangled pairs after the filter cavity is about 50 $s^{-1}\,mW^{-1}\,MHz^{-1}$. In the storage experiment, the entangled signal photons are created by a 200 ns pump pulse, which is cut from a 28 mW cw pump laser. The production rate is about 33 s^{-1}. The measured ratio of counts under $|HH\rangle/|HV\rangle$ and $|++\rangle/|+-\rangle$ bases are 14.3:1 and 23.1:1, respectively, with $|\pm\rangle = (|H\rangle \pm |V\rangle)/\sqrt{2}$.

The signal photon pair is directed to the memory lab with 20-meter single-mode fibers. The different polarization components are spatially separated by PBS_1, then transferred to right-hand circular polarized (σ^+) by wave plates, and then guided to the four quantum registers by the lens (see Fig. 2). More precisely, the $|H\rangle_1$, $|H\rangle_2$, $|V\rangle_2$, and $|V\rangle_1$ polarization components are coupled to mode 1–4, respectively. After these components enter the atomic ensemble, we adiabatically switch off the control light, and the photonic entanglement is mapped into the atomic ensemble. This yields an entanglement among the four quantum registers:

$$|\psi\rangle_a = (S^\dagger_{\mathbf{q}_1} S^\dagger_{\mathbf{q}_2} + S^\dagger_{\mathbf{q}_3} S^\dagger_{\mathbf{q}_4})|\text{vac}\rangle/\sqrt{2}.$$

After a controllable delay, we adiabatically switch on the control light and convert the atomic entanglement back into photonic entanglement. The polarization states of the output photons are transferred back linearly polarized by wave plates and combined by PBS_2 to reconstruct the biphoton entanglement. The two retrieved entangled photons are, respectively, guided into a filter consisting of a Fabry-Perot cavity (transmission window 600 MHz) and a pure ^{87}Rb vapor cell with atoms prepared in $|5S_{1/2}, F = 2\rangle$, and then detected by single-photon detectors. The measured overall average storage efficiency is shown in Fig. 3, which yields a $1/e$ lifetime of 2.8 ± 0.2 μs. The measured coincidence rate without storage and after 1 μs storage time is 1.3 s^{-1} and 0.03 s^{-1}, respectively. The propagating phase between PBS_1 and PBS_2 is actively stabilized within $\lambda_l/30$ by an additional phase lock beam with $\lambda_l \approx 780$ nm [9,28].

To verify that the biphoton Bell-type entanglement is faithfully mapped into and out of the four holographic quantum registers, we first measure the retrieved biphoton

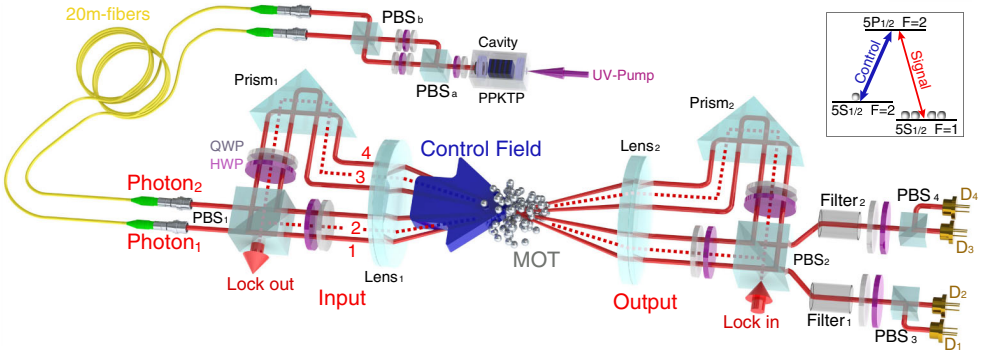

FIG. 2 (color online). Illustration of the experimental setup. The two polarization-entangled photons produced by a narrowband SPDC source are directed to the memory lab through 20 m fibers. Different polarization components are separated by the polarization beam splitter (PBS) 1, and are coupled to the quad-mode holographic quantum memory. All the light fields are turned into right-hand circular polarization (σ^+) by wave plates. The entangled photons are stored into the four quantum registers by adiabatically switching off the control light. After a controllable delay, the photons are retrieved, transferred back to their original polarization states by wave plates, and combined on PBS_2. Then the retrieved entangled photons are guided into filters, containing a Fabry-Perot cavity and a hot atomic cell to filter out the leakages from the control light, and detected by single-photon detectors. The path length difference between PBS_1 and PBS_2 is actively stabilized by an additional phase beam (dashed line). Inset: The experimental laser lights and atomic levels.

state in $|H/V\rangle$, $|\pm\rangle$, and $|R/L\rangle = (|H\rangle \pm i|V\rangle)/\sqrt{2}$ bases at different storage times. The average visibility is shown in Fig. 3, which for storage time less than 1.6 μs, exceeds the threshold of 0.71 to violate the Clauser-Horne-Shimony-Holt (CHSH)-Bell inequality [30]. Note that the reduction of the visibility with storage time is mainly due to the background coincidences caused by the dark counts and the leakage from the control field. We further measure the correlation function $E(\phi_1, \phi_2)$, with $\phi_1(\phi_2)$

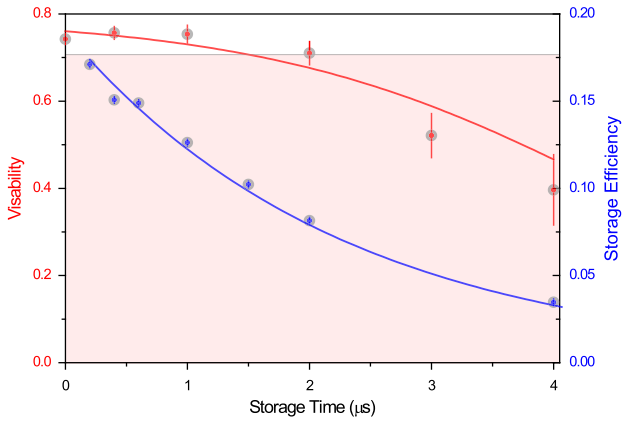

FIG. 3 (color online). Average visibility (red, left axis) and overall storage efficiency (blue, right axis) of the retrieved biphoton state versus storage time. An exponential fitting (blue [dark gray] solid line) of the storage efficiency yields a lifetime of $\tau = 2.8 \pm 0.2$ μs. The retrieved biphoton state is measured under $|H/V\rangle$, $|\pm\rangle$, and $|R/L\rangle$ bases with $|\pm\rangle = (|H\rangle \pm |V\rangle)/\sqrt{2}$, and $|R/L\rangle = (|H\rangle \pm i|V\rangle)/\sqrt{2}$. The average visibility is fitted using $V = 1/(a + be^{2t/\tau})$ (red [medium gray] solid line) with a and b the fitting parameters. The result shows that within about 1.6 μs the visibility is above the threshold of 0.71 to violate the CHSH-Bell inequality. Error bars represent $\pm$ standard deviation.

the polarization angle for signal photon 1(2), and calculate quantity $S = |-E(\phi_1, \phi_2) + E(\phi_1, \phi_2') + E(\phi_1', \phi_2) + E(\phi_1', \phi_2')|$, where $(\phi_1, \phi_1', \phi_2, \phi_2') = (0°, 45°, 22.5°, 67.5°)$. We obtain $S = 2.54 \pm 0.03$ for the input state, and $S = 2.25 \pm 0.08$ for the retrieved state after 1 μs storage. The violation of the CHSH-Bell inequality ($S > 2$) [30] confirms the entanglement has been coherently and reversibly stored in the quad-mode holographic quantum memory.

To quantitatively assess the fidelity of the storage process, we perform the quantum state tomography [31,32] to construct the density matrix ρ_{in} of the input and ρ_{out} of the output state after 1 μs storage, in which the polarization state of each photon is measured with two single-photon detectors under different detection settings. The results are illustrated in Fig. 4, from which the fidelity of the measured state ρ on the ideal Bell state ρ_{ϕ^+} is calculated as $F(\rho_{\phi^+}, \rho) = [\text{Tr}(\sqrt{\sqrt{\rho_{\phi^+}}\rho\sqrt{\rho_{\phi^+}}})]^2$. A Monte Carlo simulation technique [32] is applied to calculate the uncertainties of the fidelity. Briefly, an ensemble of 100 random sets of data are generated according to Possionian distribution and then the density matrices are obtained by means of the maximum likelihood method. This yields a distribution of fidelities, from which the mean value and uncertainties of the fidelity are calculated. We obtain $F(\rho_{\phi^+}, \rho_{\text{in}}) = (87.9 \pm 0.5)\%$ for the input state ρ_{in} and $F(\rho_{\phi^+}, \rho_{\text{out}}) = (81 \pm 2)\%$, beyond the threshold [33] of 78% for Werner states to violate the Bell inequality. The fidelity of the memory process is given by $F(\rho_{\text{in}}, \rho_{\text{out}}) = (98.2 \pm 0.9)\%$.

In summary, we have experimentally demonstrated the coherent mapping of a biphoton Bell-type entanglement, created from a narrowband SPDC source, into and out of a four-register holographic quantum memory, with a high memory-process fidelity of 98% for 1 μs storage time. The

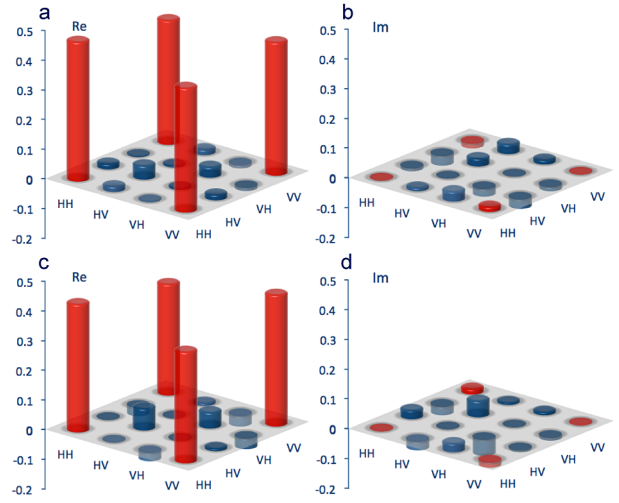

FIG. 4 (color online). Density matrix of the input state [(a), (b)] and of the output state after 1 μs storage [(c), (d)] obtained from quantum state tomography. (a) and (c) are for the real parts, and (b) and (d) are for the imaginary parts.

narrowband photonic entanglement source inherits the advantage of a conventional broadband SPDC source, and can be used to generate multiphoton entanglement beyond biphoton entanglement. A novel feature of the holographic quantum memory is that one can use more modes by simply choosing the directions of the signal and control fields. The memory capacity N_m for a coplanar configuration may be estimated by the geometric mean of the Fresnel numbers of the illuminated regions as $N_m \sim w_c w_s/(\lambda L)$ [20], which is $N_m \sim 240$ for our experimental parameters. Increasing the beam waist diameters or extending to a three-dimensional geometry would allow many more modes. Individual control of each quantum register may be achieved by using an optical cavity and employing the stimulated Raman adiabatic passage technique [18] or employing the phase match method [20].

To extend our work to the storage of multiphoton entanglement, we have to improve the brightness of the entanglement source, and increase the retrieval efficiency and lifetime of the quantum memory. The storage efficiency is about 15%, which can be improved by further increasing the optical depth and reducing the linewidth of the narrowband entanglement source. The storage time is about 1 μs, which is limited by inhomogeneous broadening induced by a residual magnetic field, and can be improved to be of the order of milliseconds by trapping the atoms in an optical lattice and using the magnetic-insensitive state [34,35]. Our work opens up the possibility of scalable preparation and high-capacity storage of multiphoton entanglement, and also sheds light on the emerging field of holographic quantum information processing.

This work was supported by the National Natural Science Foundation of China, the National Fundamental Research Program of China (Grant No. 2011CB921300), the Chinese Academy of Sciences, the Austrian Science Fund, and the European Commission through the European Research Council Grant and the Specific Targeted Research Projects of Hybrid Information Processing. H. N. D and H. Z. contributed equally to this work.

*eidos@ustc.edu.cn
†bozhao@ustc.edu.cn

[1] E. Knill, R. LafLamme, and G. J. Milburn, Nature (London) **409**, 46 (2001).
[2] L.-M. Duan, M. D. Lukin, J. I. Cirac, and P. Zoller, Nature (London) **414**, 413 (2001).
[3] B. Julsgaard, J. Sherson, J. I. Cirac, J. Fiurášek and E. S. Polzik, Nature (London) **432**, 482 (2004).
[4] J. Appel, E. Figueroa, D. Korystov, M. Lobino, and A. I. Lvovsky, Phys. Rev. Lett. **100**, 093602 (2008).
[5] T. Chanelière, D. N. Matsukevich, S. D. Jenkins, S.-Y. Lan, T. A. B. Kennedy, and A. Kuzmich, Nature (London) **438**, 833 (2005).
[6] M. D. Eisaman, A. André, F. Massou, M. Fleischhauer, A. S. Zibrov, and M. D. Lukin, Nature (London) **438**, 837 (2005).
[7] K. S. Choi, H. Deng, J. Laurat, and H. J. Kimble, Nature (London) **452**, 67 (2008).
[8] K. S. Choi, A. Goban, S. B. Papp, S. J. van Enk, and H. J. Kimble, Nature (London) **468**, 412 (2010).
[9] H. Zhang *et al.*, Nature Photon. **5**, 628 (2011).
[10] C. Clausen, I. Usmani, F. Bussières, N. Sangouard, M. Afzelius, H. de Riedmatten, and N. Gisin, Nature (London) **469**, 508 (2011).
[11] E. Saglamyurek *et al.*, Nature (London) **469**, 512 (2011).
[12] H. P. Specht, C. Noelleke, A. Reiserer, M. Uphoff, E. Figueroa, S. Ritter, and G. Rempe, Nature (London) **473**, 190 (2011).
[13] S.-Y. Lan, A. G. Radnaev, O. A. Collins, D. N. Matsukevich, T. A. Kennedy, and A. Kuzmich, Opt. Express **17**, 13 639 (2009).
[14] J. Nunn, K. Reim, K. C. Lee, V. O. Lorenz, B. J. Sussman, I. A. Walmsley, and D. Jaksch, Phys. Rev. Lett. **101**, 260502 (2008).
[15] E. Zeuthen, A. Grodecka-Grad, and A. S. Sørensen, Phys. Rev. A **84**, 043838 (2011).
[16] M. Hosseini, B. M. Sparkes, G. Hétet, J. J. Longdell, P. K. Lam, and B. C. Buchler, Nature (London) **461**, 241 (2009).
[17] H. de Riedmatten, M. Afzelius, M. U. Staudt, C. Simon, and N. Gisin, Nature (London) **456**, 773 (2008).
[18] K. Tordrup, A. Negretti, and K. Mølmer, Phys. Rev. Lett. **101**, 040501 (2008).
[19] D. V. Vasilyev, I. V. Sokolov, and E. S. Polzik, Phys. Rev. A **77**, 020302 (2008).
[20] K. Surmacz, J. Nunn, K. Reim, K. C. Lee, V. O. Lorenz, B. Sussman, I. A. Walmsley, and D. Jaksch, Phys. Rev. A **78**, 033806 (2008).
[21] M. Fleischhauer and M. D. Lukin, Phys. Rev. Lett. **84**, 5094 (2000).
[22] C. Liu, Z. Dutton, C. H. Behroozi, and L. V. Hau, Nature (London) **409**, 490 (2001).
[23] D. F. Phillips, A. Fleischhauer, A. Mair, R. L. Walsworth, and M. D. Lukin, Phys. Rev. Lett. **86**, 783 (2001).

[24] N. B. Phillips, A. V. Gorshkov, and I. Novikova, Phys. Rev. A **78**, 023801 (2008).
[25] P. K. Vudyasetu, R. M. Camacho, and J. C. Howell, Phys. Rev. Lett. **100**, 123903 (2008).
[26] M. Shuker, O. Firstenberg, R. Pugatch, A. Ron, and N. Davidson, Phys. Rev. Lett. **100**, 223601 (2008).
[27] H. Wu *et al.*, Phys. Rev. Lett. **105**, 140503 (2010).
[28] S. Chen, Y.-A. Chen, B. Zhao, Z.-S. Yuan, J. Schmiedmayer, and J.-W. Pan, Phys. Rev. Lett. **99**, 180505 (2007).
[29] X.-H. Bao, Y. Qian, J. Yang, H. Zhang, Z.-B. Chen, T. Yang, and J.-W. Pan, Phys. Rev. Lett. **101**, 190501 (2008).
[30] J. F. Clauser, M. A. Horne, A. Shimony, and R. A. Holt, Phys. Rev. Lett. **23**, 880 (1969).
[31] G. M. D'Ariano, M. G. A. Paris, and M. F. Sacchi, Adv. Imaging Electron Phys. **128**, 205 (2003).
[32] J. B. Altepeter, E. R. Jeffrey, and P. G. Kwiat, Adv. At. Mol. Opt. Phys. **52**, 105 (2005).
[33] M. Aspelmeyer *et al.*, Science **301**, 621 (2003).
[34] B. Zhao *et al.*, Nature Phys. **5**, 95 (2009).
[35] R. Zhao, Y. O. Dudin, S. D. Jenkins, C. J. Campbell, D. N. Matsukevich, T. A. B. Kennedy, and A. Kuzmich, Nature Phys. **5**, 100 (2009).